

Polymer blends of polyamide-6 (PA6) and poly(phenylene oxide) (PPO) compatibilized by styrene–maleic anhydride (SMA) copolymer

Chih-Rong Chiang and Feng-Chih Chang*

Institute of Applied Chemistry, National Chiao-Tung University, Hsinchu, Taiwan, Republic of China

(Received 19 December 1996)

The commercially available styrene–maleic anhydride copolymer (SMA–8% MA) has been demonstrated to be a highly effective compatibilizer for polymer blends of polyamide-6 (PA6) and poly(2,6-dimethyl-1,4-phenylene oxide) (PPO). SMA is miscible with PPO and tends to be dissolved in the PPO phase during the earlier stages of melt blending. The dissolved SMA has the chance to make contact and reacts with PA6 at the interface to form the desirable SMA-*g*-PA6 copolymer. This *in situ*-formed SMA-*g*-PA6 graft copolymer tends to anchor along the interface to reduce the interfacial tension and results in finer phase domains. The overall mechanical property improvement of the compatibilized blends over the uncompatibilized counterparts is drastic, especially for these PPO-rich blends. The mechanism of this conventional reactive compatibilization system has been discussed in detail. © 1997 Elsevier Science Ltd.

(Keywords: blend; polyamide-6; PPO; SMA; compatibilizer)

INTRODUCTION

Polyamide (PA) (nylon) is one of the important classes of polymer for engineering applications, with excellent chemical resistance. However, poor dimensional stability and low impact strength are deficiencies of unmodified nylons. On the other hand, poly(phenylene oxide) (PPO) exhibits high dimensional stability and good thermal properties. However, PPO also has a number of deficiencies such as poor solvent resistance and difficulty in processing. The inherent properties of nylon and PPO suggest that a combination of PA and PPO would produce materials with balanced properties provided that the advantages of one component can compensate for the deficiencies of the other. Polymer blends of nylon and PPO have attracted great interest from both industry and academia.

Numerous papers have reported the use of maleic anhydride-containing copolymers as compatibilizers for blends of PA and PPO^{1–16}. Campbell *et al.*^{1,2} reported ductility improvements of PA66/PPO blends with a styrene–ethylene, butylene–styrene (SEBS) impact modifier by addition of an anhydride-functionalized PPO copolymer, resulting in an enormous reduction of the size of dispersed PPO particles. Hobbs *et al.*^{3,4} studied the PA66/PPO/styrene–butadiene–styrene copolymer (SBS) blends by addition of a proprietary copolymer as a compatibilizer. PA66 forms the continuous phase while the rubbery impact modifier is contained within the dispersed PPO domains. Nishio *et al.*^{5–7} reported that

maleic anhydride-grafted ethylene/propylene rubber can function as a mutual compatibilizer for blends of PA and PPO. Gallucci⁸ studied PA/PPO blends compatibilized by a maleic anhydride-grafted SEBS and reported improvement in toughness of the blends. Laverty *et al.*⁹ studied the recyclability of PA66/PPO alloys by examining the effects of multiple melt processes upon the impact strength. The reducing properties of the multiple melt processed PA66/PPO blends are due to the coalescence of PPO particles. Ghidoni *et al.*¹⁰ reported that blending N-methyl-4-nitro-phthalimide functionalized PPO with PA modified with a rubber results in a remarkable improvement of the impact strength relative to the uncompatibilized counterparts. Akkapeddi *et al.*¹¹ found a significant difference in the relative reactivity of the anhydride-functionalized PPO and the PA during extrusion blending, which could be correlated to the backbone and end group structure of PA. Lai¹² used PA-*g*-PPO graft copolymers as compatibilizers for PA6/PPO blends. The PA6/PPO blends with 10% grafted copolymer show satisfactory mechanical properties except for tensile elongation. Chiang and Chang¹³ reported that styrene-co-glycidyl methacrylate copolymer functions as an effective compatibilizer for PA/PPO blends, with substantial improvements in mechanical properties. Several Japanese patents^{14–16} claimed SMA copolymers as efficient compatibilizers for PA/PPO blends by improving heat deflection temperature and solvent resistance.

In this study, we intend to report in details on PA6/PPO blends compatibilized by a commercially available SMA copolymer.

* To whom correspondence should be addressed

EXPERIMENTAL

Material

The PA6 used in this study is a commercial product, Novamid 1010C2, produced by Mitsubishi Kasei Co Ltd of Japan. The SMA copolymer containing 8 wt% maleic anhydride, Dylark 232, was obtained from Arco Co. Unmodified PPO powder was purchased from General Electric Co and has an intrinsic viscosity of 0.4 dl g^{-1} , measured in chloroform at 25°C .

Blend preparation

All the blends were prepared on a co-rotating 30 mm twin-screw extruder ($L/D = 36$, Sino-Alloy Machinery Inc.) with a rotational speed of 280 rpm. Vacuum was applied in the decompression zone. The barrel temperatures were set from 210 to 290°C . Standard ASTM 1/8 inch testing specimens were prepared by an Arburg 3 oz injection moulding machine. The temperatures of injection moulding were adjusted to optimize the processing conditions, depending on the compositions. The detailed processing conditions for the extrusion and injection moulding are listed in Table 1.

Characterization

Fourier transform infra-red spectroscopy (FT i.r.) analyses were carried out using a Nicolet 500 Infrared Spectrophotometer.

Capillary rheological measurements of the blends and neat components were carried out at 270°C using a Kayness Galaxy Capillary Rheometer with a die orifice radius of 0.04 inch and a die length of 0.8 inch.

The morphologies of the injection moulded specimens were examined using a Hitachi S-570 scanning electron microscope (SEM) at an accelerating voltage of 20 kV. Cryogenically fractured surfaces of the moulded specimens were coated with a thin film of gold prior to SEM examination.

Dynamic mechanical analysis (d.m.a.) was performed using a Du Pont 983 scanning d.m.a. unit from -50 to 250°C .

Tensile tests were conducted at ambient conditions

using an Instron universal testing machine, Model 4201, according to ASTM D638. The cross-head speed was 5 mm min^{-1} . Unnotched Izod impact strengths were measured at ambient conditions according to the ASTM-D256 method. After injection moulding and prior to test, specimens were conditioned in the laboratory atmosphere for a minimum of 7 days.

Annealing was carried out at 200°C for 60 min in a temperature-controlled oven.

RESULTS AND DISCUSSION

Chemistry

A reactive compatibilizer is a copolymer with reactive functional groups that are able to react with one or both of the blend components to form block or graft copolymers. These *in situ*-formed copolymers tend to reside at the interface to compatibilize the blend. Reactive copolymers undergo the usual chemical reactions seen in low-molecular-weight materials. However, the reactions involving the functional groups in macromolecules are more complex than those of low-molecular-weight materials. The major chemical reactions involved in this reactive compatibilized blend system involve the anhydride groups of the SMA copolymer and the terminal amine groups of PA6^{17,18}. The chemistry of the reactions is shown in Figure 1. The amic acid formed initially in this reaction is eventually converted to the heat-stable succinimide group during melt processing. The *in situ*-formed SMA-g-PA6 copolymer is located preferentially at the interface to act as an effective compatibilizer.

Fourier transform infra-red spectroscopy (FT i.r.)

The formation of the *in situ*-formed graft copolymers was characterized by FT i.r. The characteristic absorption bands of SMA at 1781 and 1857 cm^{-1} are the carbonyl resonance by the maleic anhydride group¹⁷, as shown in Figure 2(a). The ring stretching of styrene occurs at the absorption band of 1601 cm^{-1} . Figure 2(b) shows $\nu_{\text{C=O}}$ stretching and $\nu_{\text{N-H}}$ bending of the PA6 at 1662 and 1631 cm^{-1} , respectively¹⁹.

Table 1 Processing conditions

A. Extrusion conditions											
Composition			Barrel temperature ($^\circ\text{C}$)								
PA6	PPO	Stage: 1	2	3	4	5	6	7	8	9	Die
70	30	210	245	265	270	275	275	270	270	265	265
50	50	210	255	275	285	285	280	280	275	275	275
30	70	210	260	275	290	290	290	285	285	285	285
Screw speed: 260 rpm Feeding rate: 145 g min^{-1}											
B. Injection conditions											
Composition			Barrel temperature ($^\circ\text{C}$)								
PA6	PPO	Stage: 1	2	3	Nozzle			Mould temperature ($^\circ\text{C}$)			
70	30	245	255	265	265			80			
50	50	255	265	275	285			100			
30	70	280	290	300	300			120			

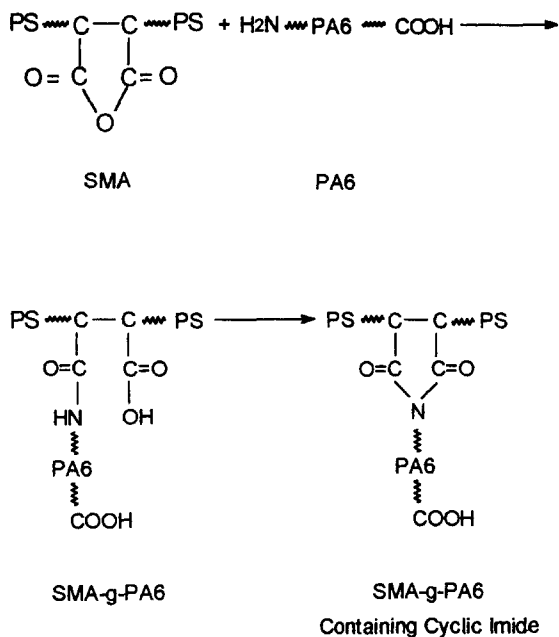


Figure 1 Scheme of maleic anhydride/amine reaction

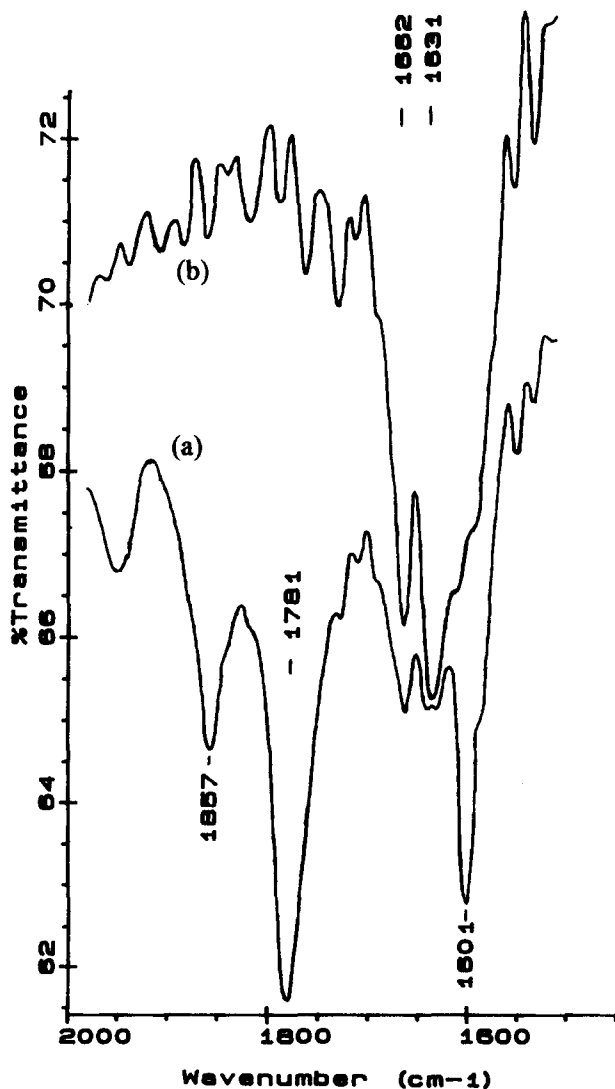


Figure 2 Infra-red spectra of neat components: (a) SMA; (b) PA6

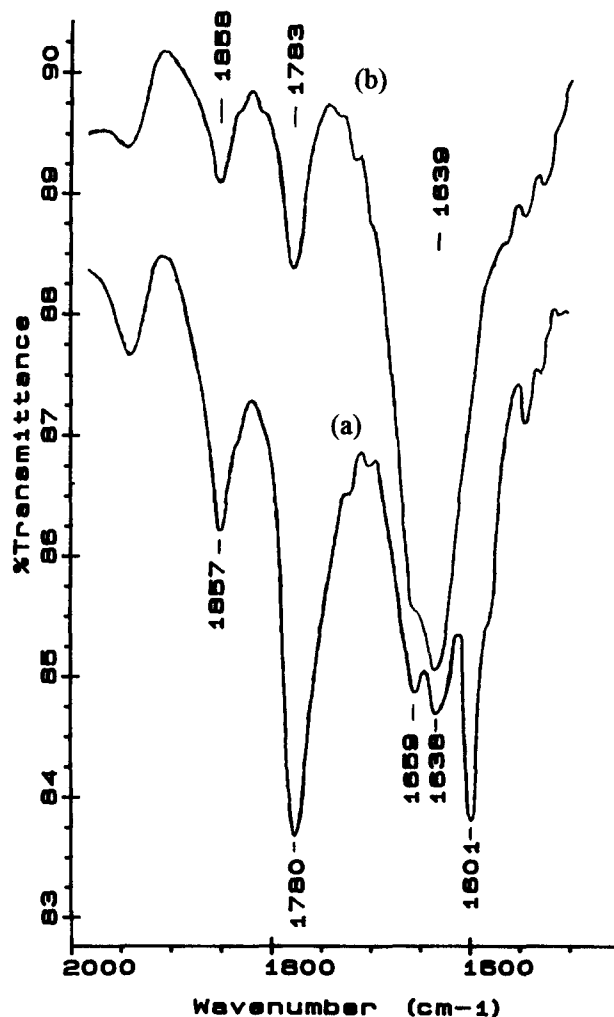


Figure 3 Infra-red spectra of mixtures: (a) dry-blended PA6/SMA = 1/1 mixture; (b) melt-blended PA6/SMA = 1/1 mixture

Figure 3 compares the FT i.r. spectra of the mixtures of PA6 and SMA by dry mixing and melt blending. No reaction is expected for the dry-mixed PA6/SMA blend that shows the characteristic bands from the neat PA6 (1659 and 1638 cm^{-1}) and the neat SMA (1601, 1780 and 1857 cm^{-1}) (Figure 3(a)). The area and shape of the characteristic peaks of maleic anhydride from the dry-blended mixture (Figure 3(a)) are similar to those from the neat SMA (Figure 2(a)). Comparing Figures 3(a) and 3(b), the areas of the SMA characteristic peaks at 1781 and 1857 cm^{-1} of the melt-blended mixture are significantly smaller than those of the dry-blended mixture. The reduction of these maleic anhydride characteristic peaks observed after melt blending indicates that the reaction of maleic anhydride with amine indeed occurs.

Scott and Macosko¹⁷ have reported that the maleic anhydride/amine reaction by forming a cyclic imide can be easily detected by i.r. at 1771 and 1701 cm^{-1} . In this study, the expected peak at 1771 cm^{-1} is overlapped with the peak from SMA at 1781 cm^{-1} while the peak at 1701 cm^{-1} is covered by the PA6 broad peak at 1639 cm^{-1} and the styrene ring absorption band of the SMA. Therefore we are unable to positively identify the formation of the cyclic imide.

From the above evidence, we can expect that the reaction between SMA and PA6 to form SMA-g-PA6

copolymers through the maleic anhydride/amine reaction indeed occurs.

Capillary rheometry

The shear viscosity *versus* shear rate behaviours of pure components and PA-rich PA6/PPO = 70/30 blends, with and without compatibilizer, at 270°C are shown in Figure 4. All molten polymers show non-Newtonian flow behaviour. Rheological data from the neat PPO could not be obtained because its viscosity at 270°C is above the measuring limit of the instrument. Within the range of shear rates investigated, the SMA copolymer exhibits substantially more shear-thinning than the rest.

The effect of the compatibilizer SMA on the viscosity of the PA6/PPO blend is very complex, including at least three major factors: (a) phase structural transformation, (b) molecular weight increase and interfacial friction increase, and (c) plasticizing of PPO by unreacted or lightly reacted SMA. It has been reported that the SMA copolymer with 8% maleic anhydride is fully miscible with PPO^{20,21}. SMA, similarly to polystyrene, is dissolved in the PPO phase as a plasticizer and reduces the intrinsic viscosity of this phase. The viscosity of this

PA6/PPO = 70/30 series increases with increase of the SMA content, as shown in Figure 4. The phase structural transformation plays a less important or no role in this series of blends because PPO is the dispersed phase regardless of the amount of SMA in the blend. It appears that the molecular weight increase and higher interfacial friction by the graft reaction is more important than plasticization and dominates the final viscosity of this series of blends. Plasticizing of PPO by SMA is effective only for those unreacted SMA molecules. A similar increase in viscosity was also observed for PA/PP blends using a maleic anhydride functionalized compatibilizer²².

Figure 5 shows the plots of the viscosity *versus* shear rate of this interesting PA6/PPO = 50/50 series. The viscosity of the uncompatibilized blend (Curve A) is the highest, while the one with lowest viscosity is the blend containing 2 phr SMA (Curve B). The viscosity increases with increase of SMA content but is still lower than that of the uncompatibilized blend, as shown in Figure 5. The observed highest viscosity from the uncompatibilized blend is probably due to the extremely high viscosity of the PPO in a nearly co-continuous phase structure. However, the morphology of the injection moulded specimen of this uncompatibilized PA6/PPO = 50/50

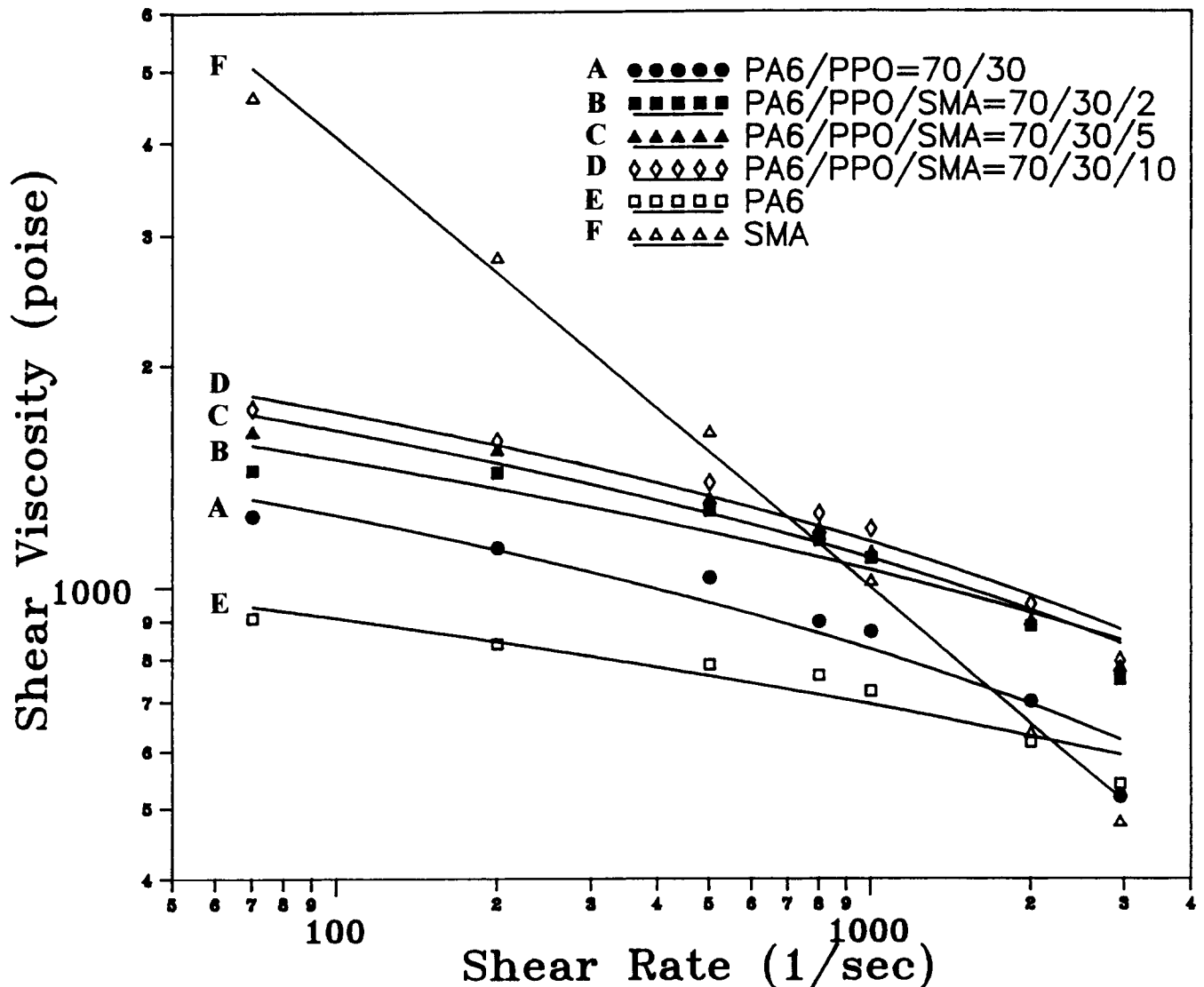


Figure 4 Plots of shear viscosity vs shear rate at 270°C for PA6, SMA and various PA6/PPO = 70/30 blends

blend (Figure 9A) gives large PPO particles with PA6 inclusion rather than an as expected co-continuous structure. We believe that these large PPO particles are the result of relaxation and coalescence after injection moulding, which does not represent the true co-continuous phase structure of a high shear capillary rheometer die string.

The addition of 2 phr SMA or higher in the PA6/PPO = 50/50 blend clearly transforms the blend phase structure into a PPO droplet morphology (Figures 9B and 9C) and therefore the phase transformation has no role in dictating the viscosity. For the blends containing 2 phr SMA or higher, the viscosity is determined by competition between the molecular weight increase and the plasticization. The observed trend of increase in viscosity with increase of SMA content implies that the molecular weight increase dominates the final viscosity.

Figure 6 shows a very unusual phenomenon where essentially all the viscosity *versus* shear rate curves from the PA6/PPO = 30/70 series are nearly overlapped. Morphological data (Figure 10) clearly show the gradual phase structural transformation from co-continuous to PPO dispersed particles with the increase of SMA content. Competition among the above-mentioned

three factors results in nearly equal viscosity of the uncompatibilized and compatibilized PA6/PPO = 30/70 blends, as shown in Figure 6.

Dynamic mechanical analysis (d.m.a.)

The dynamic mechanical behaviour of the PA6/PPO = 30/70 series is shown in Figure 7. Both uncompatibilized and compatibilized blends give two glass transition temperatures, indicating phase separation of the blend components. The uncompatibilized PA6/PPO = 30/70 blend shows a very sharp T_g transition at 238.9°C for the PPO phase and a PA6 T_g transition at 51.5°C (Figure 7A). This detected T_g of PPO is substantially higher than values reported in the literature, which is probably due to the instrument calibration problem. The PPO peak of the PA6/PPO/SMA = 30/70/1 blend (Figure 7B) is still very sharp and its T_g is close to the predicted miscible value calculated by the Fox equation. The PA6 T_g peak (Figure 7B) shifts to high temperature only slightly (0.8°C) because of the relatively smaller amount of SMA-g-PA6 copolymers produced.

The PPO T_g transition behaviour of the compatibilized blends containing higher SMA content (more than

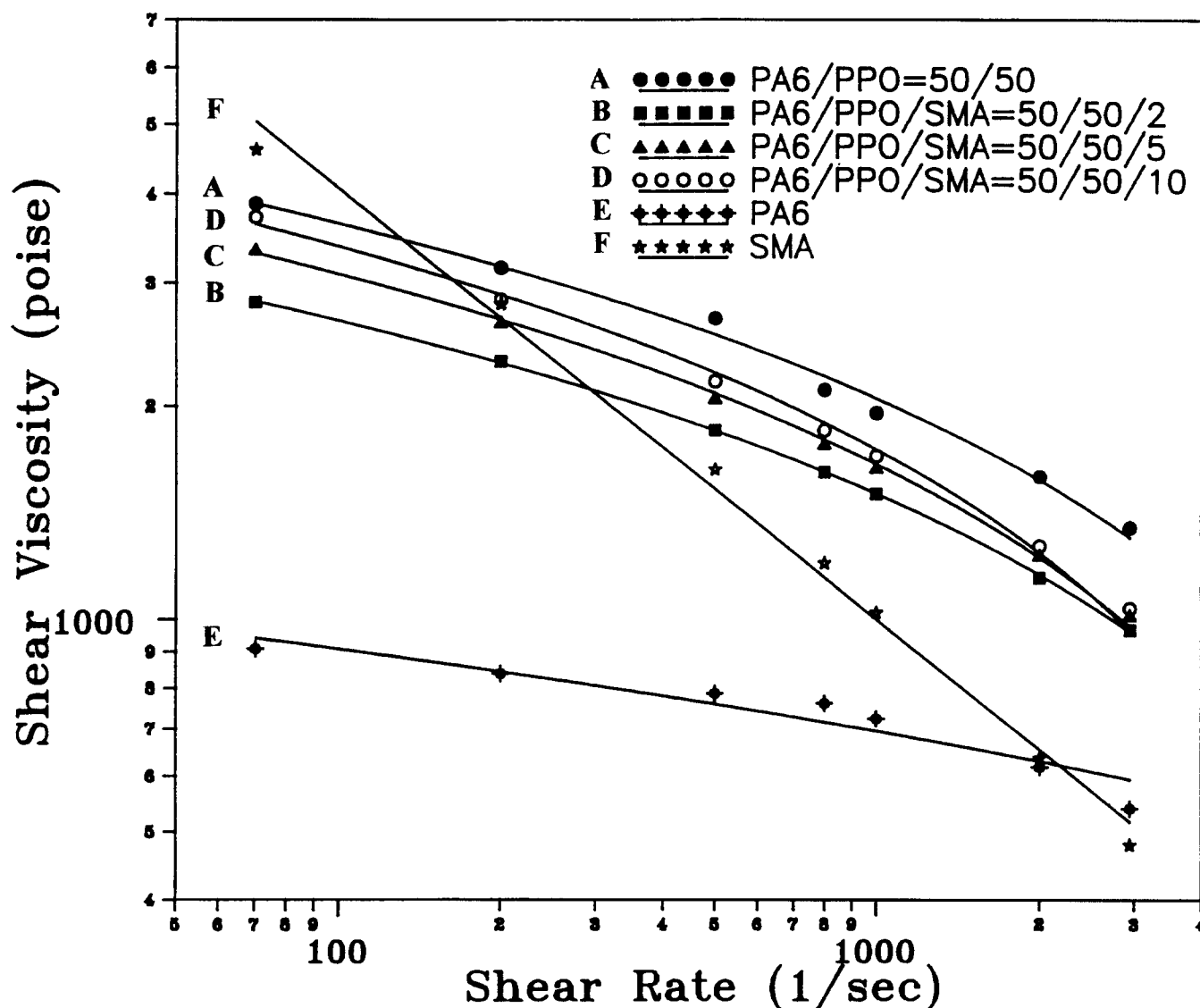


Figure 5 Plots of shear viscosity vs shear rate at 270°C for PA6, SMA and various PA6/PPO = 50/50 blends

2 phr) is somewhat different; the peak broadens and shifts toward lower temperatures substantially, as shown in *Figures 7C, 7D, 7E* and *Table 2*. The shape of the PA6 T_g transition peak remains the same as that of the uncompatibilized blend, whereas the PA6 T_g peak shifts slightly to a higher temperature with the increase of the quantity of SMA. SMA has a T_g (120°C) between that of PA6 and PPO. The dissolved free SMA copolymer in the PPO phase is responsible for the substantially lower PPO T_g observed. The distribution of the SMA-g-PA6 copolymer molecules along the interface is responsible for the PPO transition peak broadening. A small quantity of SMA-g-PA6 copolymer is expected to be distributed in the PA6 phase, causing only a slight increase in its T_g .

Morphologies

Melt-blended immiscible polymer blends possess complicated phase morphologies which depend on interfacial tension, viscosity ratio of blend constituents, volume fraction, and processing conditions. Pieces of one polymer may be drawn into filaments which may remain as filaments, break up into smaller droplets, or connect with each other to give an interconnected network.

SEM photomicrography is the most convenient approach to differentiate the morphologies between the compatibilized and the uncompatibilized blends. The incompatible blend possesses higher interfacial tension and usually results in coarser morphology than that of the corresponding compatibilized blend. *Figure 8* shows the unetched SEM micrographs of the PA6/PPO = 70/30 series blends. The addition of 5 phr SMA compatibilizer reduces the domain size of the PPO dispersed particles, but not very substantially. This is probably due to significantly higher viscosity of the dispersed phase (PPO) relative to that of the matrix (PA6). *Figure 9* gives the etched micrographs of the PA6/PPO = 50/50 series where the PA6 is also the continuous phase. The uncompatibilized PA6/PPO = 50/50 blend (*Figure 9A*) shows that the large PPO particles have inclusions of PA6 particles. This phenomenon is probably caused by the relaxation and coalescence of the originally elongated PPO domains, encapsulating the surrounding PA6 domains due to the incompatibility of the blend. After SMA compatibilization, reduced interfacial tension results in finer and more stable phase domains (*Figures 9B and 9C*). Coalescence of the PPO dispersed phase is essentially non-existent and results in fine and stable morphology.

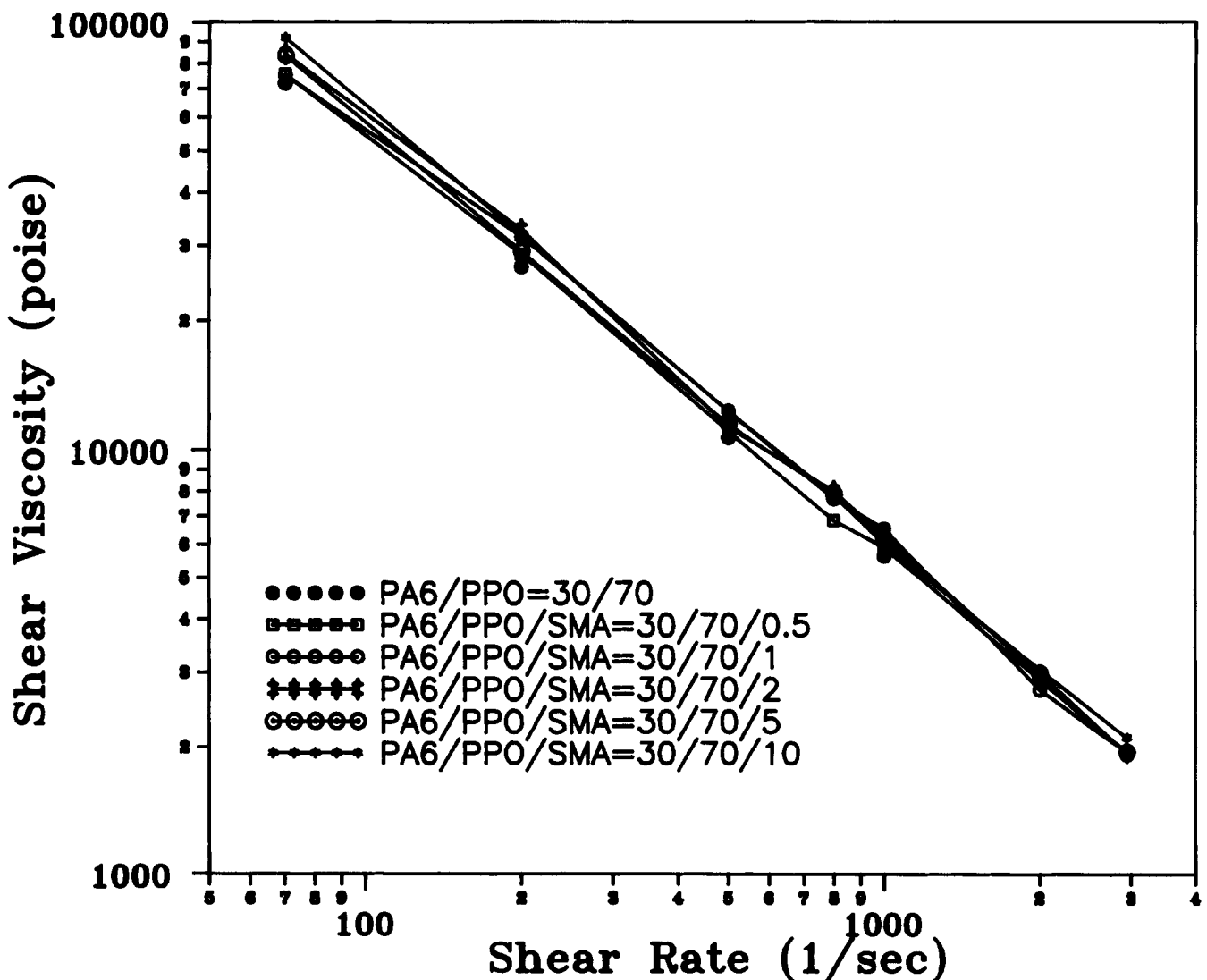


Figure 6 Plots of shear viscosity vs shear rate at 270°C for uncompatibilized and compatibilized PA6/PPO = 30/70 blends

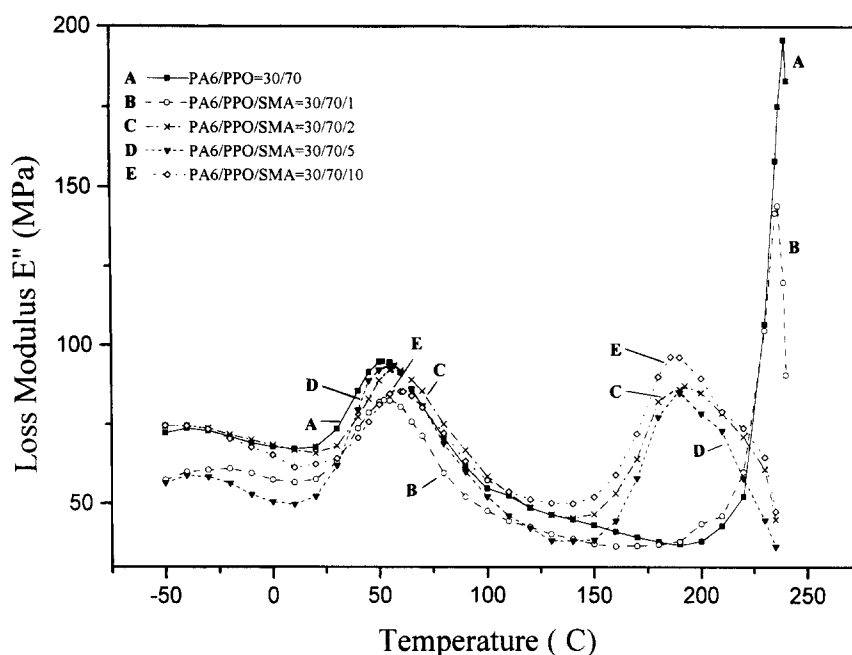


Figure 7 D.m.a. spectra of uncompatibilized and compatibilized PA6/PPO = 30/70 blends

Table 2 Transition temperatures of PA6/PPO = 30/70 blends

Composition			Transition temperature (°C)	
PA6	PPO	SMA	Tg1	Tg2
30	70	0	51.5	238.9
30	70	1	52.3	236.3
30	70	2	57.3	192.4
30	70	5	56.9	189.7
30	70	10	61.1	190.0

Figure 10 illustrates the micrographs of the PA6/PPO = 30/70 series. The uncompatibilized PA6/PPO = 30/70 blend (Figure 10A) shows a co-continuous phase structure, even though the PA6 is the minor component in the blend, but PA6 has significantly lower viscosity than PPO. Figures 10B and 10C show that the blends containing 0.5 and 1.0 phr SMA also possess a nearly co-continuous morphology but tend to shift into PPO as the dispersed phase with PA6 is included. The size of the PA6-included PPO particles is reduced after compatibilization. The presence of 2.0 phr SMA in the blend results in the most drastic morphology change (compare Figures 10C and 10D). The PPO coalescence has virtually disappeared and the PPO exists as very fine particles distributed within the PA6 phase. It is interesting to point out here that PA6 is the minor component in this blend but tends to shift from being a co-continuous phase into a continuous matrix as the quantity of compatibilizer is increased. By adding 10 phr SMA, the morphology of the blend is made extremely fine and the very fine PPO particles are evenly distributed (Figure 10E). The presence of SMA compatibilizer can affect the morphologies of these PA6/PPO blends in many ways, such as: (a) shifting a co-continuous phase structure to PPO as dispersed domains, (b) reducing interfacial tension and resulting in finer phase domains, (c) reducing or preventing phase coalescence, and (d) reducing



A. PA6/PPO=70/30

B. PA6/PPO/SMA=70/30/5

Figure 8 Unetched SEM micrographs of uncompatibilized and compatibilized PA6/PPO = 30/70 blends

viscosity mismatch by plasticizing the viscous PPO phase.

Mechanical properties

Summarized mechanical properties of the unannealed and annealed blends, including tensile properties and unnotched Izod impact strength, are shown in Table 3 and Figures 11–13. All the PA6/PPO blends, uncompatibilized or compatibilized, are brittle with nearly the same low notched impact strength because both PA6 and PPO matrices are notch sensitive. Unnotched impact strength is commonly used to differentiate toughness change resulting from compatibilization. Unnotched Izod impact value, plotted as a function of compatibilizer content (phr), is shown in Figure 11. The improvement of impact strength by the SMA compatibilizer is dramatic, especially for the PPO-rich blends. For the PA6-dominant blends (PA6/PPO = 70/30), the impact strength increases gradually with increasing quantity of SMA. The effect of SMA compatibilizer on impact strength of the PA6/PPO = 30/70 blend series is striking;

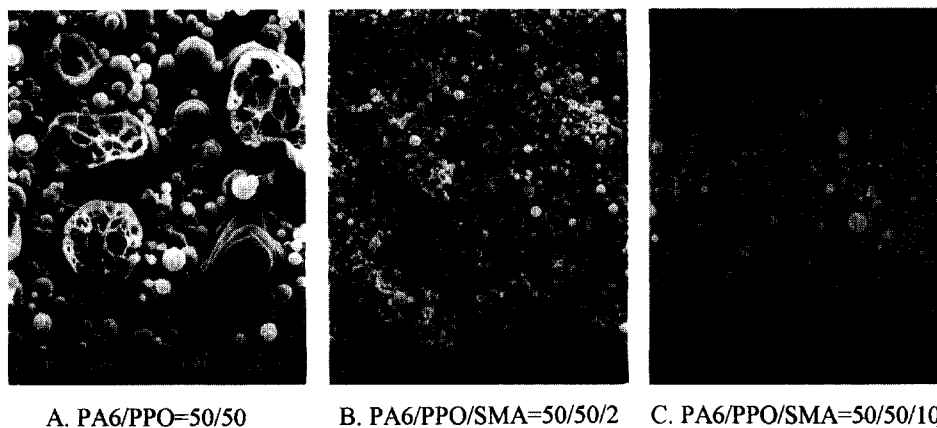


Figure 9 Etched SEM micrographs of uncompatibilized and compatibilized PA6/PPO = 50/50 blends

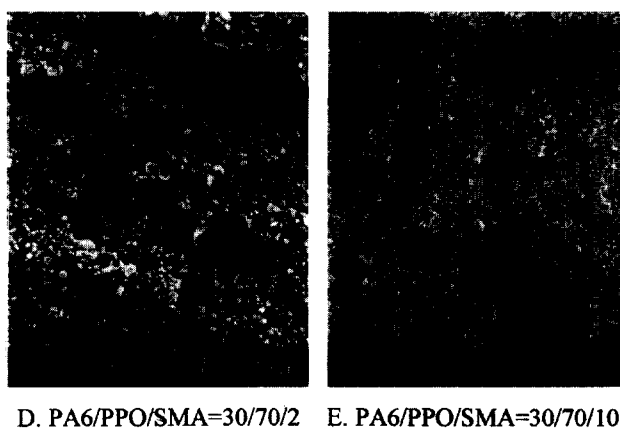
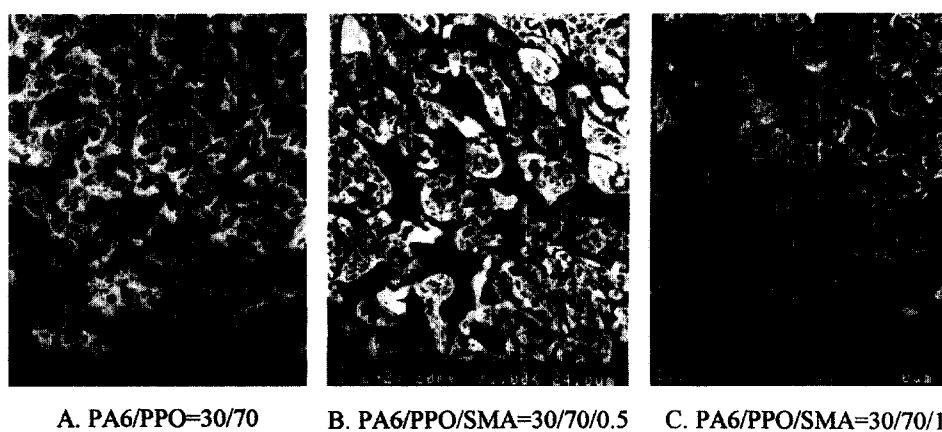


Figure 10 Etched SEM micrographs of uncompatibilized and compatibilized PA6/PPO = 30/70 blends

the impact strength increases by about 500% when the SMA content is increased from 0 to 10 phr.

Figure 12 illustrates the effect of the quantity of SMA on the resultant tensile strength of the PA6/PPO blends. The improvement of the tensile strength is also very drastic as a result of compatibilization. Two phr compatibilizer is able to approach the maximum achievable value.

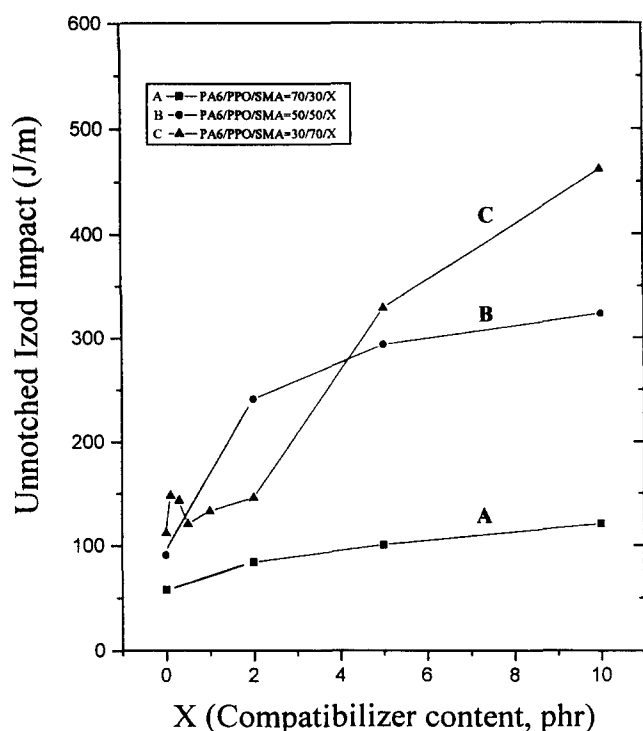
Figure 13 again demonstrates a substantial improvement in the tensile elongation of the compatibilized blends. The trend of the elongation improvement is similar to that of impact strength; the improvement of the PPO-rich blends is again more substantial than that

of the PA6-rich blends. The moduli of the compatibilized blends are also higher than those of the corresponding uncompatibilized blends, but the extent of the increase is relatively less. The annealed specimens result in higher tensile strength but lower tensile elongation and impact strength relative to their unannealed counterparts, as would be expected (Table 3).

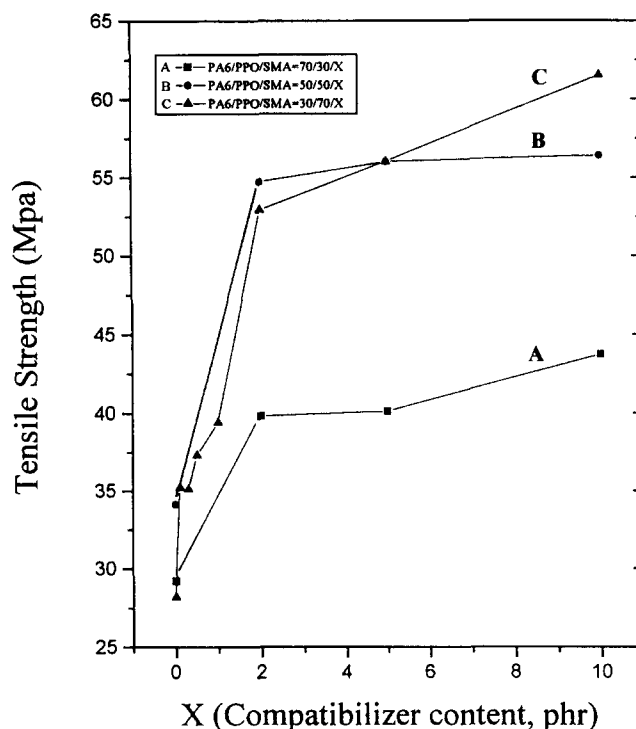
A compatibilized polyblend, in general, has finer phase domain size, greater interfacial contact area and higher interfacial adhesion than that from the corresponding uncompatibilized blend. The addition of SMA compatibilizer results in improved compatibility between PA6 and PPO, reflecting in an improvement of the mechanical

Table 3 Mechanical properties of PA6/PPO/SMA blends

Composition	Tensile strength (MPa)	Elongation (%)	Modulus (MPa)	Unnotched Izod impact (J/M)
PA6/PPO = 70/30	29.2	2.1	1530	57.5
PA6/PPO/SMA = 70/30/2	39.8	2.7	1570	83.8
PA6/PPO/SMA = 70/30/5	40.1	2.9	1650	100
PA6/PPO/SMA = 70/30/10	43.7	3.2	1660	121
PA6/PPO = 50/50	34.1	3.0	1690	90.6
PA6/PPO/SMA = 50/50/2	54.7	4.2	1690	241
PA6/PPO/SMA = 50/50/5	56.0	4.6	1700	293
PA6/PPO/SMA = 50/50/10	56.4	4.8	1760	323
PA6/PPO = 30/70	28.2	2.5	2140	111
PA6/PPO/SMA = 30/70/0.1	35.2	2.5	2150	147
PA6/PPO/SMA = 30/70/0.3	35.1	2.4	2180	143
PA6/PPO/SMA = 30/70/0.5	37.3	2.6	2230	120
PA6/PPO/SMA = 37/70/1	39.4	2.8	2250	132
PA6/PPO/SMA = 37/70/2	52.9	3.9	2170	145
PA6/PPO/SMA = 37/70/5	56.0	4.2	2280	328
PA6/PPO/SMA = 37/70/10	61.5	6.7	2320	461

**Figure 11** Effect of compatibilizer quantity on impact strength of PA6/PPO blends

properties of the blend. Mechanical property improvement comes from *in situ*-formed SMA-g-PA6 copolymer molecules anchoring along the interface. A greater quantity of SMA tends to form greater numbers of SMA-g-PA6 copolymer molecules anchoring along the interface. The SMA and PA6 segments of the SMA-g-PA6 copolymer at the interface mix intimately with the respective PPO and PA6 phases. SMA has been demonstrated to be an excellent reactive compatibilizer for PA6/PPO blends on the basis of drastic improvement in their mechanical properties.

**Figure 12** Effect of compatibilizer quantity on tensile strength of PA6/PPO blends

Compatibilization mechanism

A non-reactive compatibilizer is usually a non-reactive block or graft copolymer possessing segments structurally similar to or miscible with the blend constituents. The mechanism of a reactive compatibilizer is much more complicated because the chemical structure, its quantity, and the final location of the *in situ*-formed copolymer vary with processing condition, reactive group concentration and blending sequence. This PA6/PPO blend compatibilized by SMA is a conventional type of reactive compatibilization. The MA groups in the

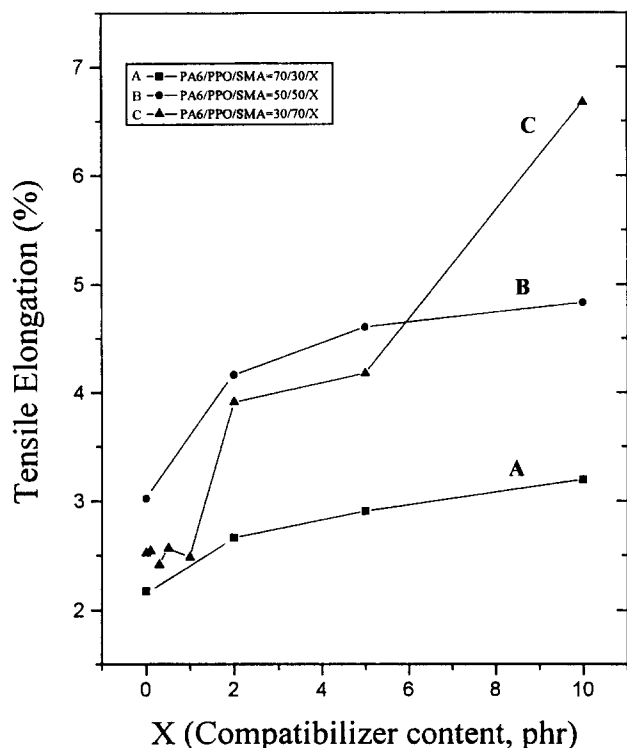


Figure 13 Effect of compatibilizer quantity on tensile elongation of PA6/PPO blends

SMA copolymer are capable of a chemical reaction with the PA6 terminal amine group to form various SMA-g-PA6 graft copolymers. The graft reaction may take place more than once per SMA main chain, depending on processing condition and blending sequence. Since this SMA (8% MA) is thermodynamically miscible with PPO, it tends to be dissolved into PPO in a one-step blending with PA6 and PPO simultaneously.

A fraction of the dissolved SMA may not have the chance to make contact and react with PA6 at the interface during melt blending. The substantial PPO T_g drop of the SMA compatibilized PA6/PPO blends by DMA (Figure 7) provides strong evidence for dissolved free SMA in the PPO phase. A fraction of the dissolved SMA has the opportunity to make contact and react with PA6 to form the desirable SMA-g-PA6 copolymer at the interface, depending on the amount of SMA employed during the vigorous melt blending. Most of the *in situ*-formed SMA-g-PA6 copolymer molecules at interface are believed to be only lightly grafted, one or two grafts per SMA main chain, because the rest of the SMA segment is miscible with PPO and tends to mix intimately with the PPO phase. Lightly grafted copolymer, with one to two grafts per main chain, has been demonstrated to be the most efficient compatibilizer^{23,24}. Prolonging the time of melt blending may cause additional grafting at the interface and such excessively grafted copolymer is considered less effective as a compatibilizer. This excessive grafting tends to happen if the SMA contains a high MA concentration. As mentioned previously^{24,25}, reactive group concentration is an important factor in designing an optimized compatibilization system. Too high an MA concentration in SMA may produce an excessively grafted comb-like copolymer. This copolymer has the PA6 grafted chains effectively shielding off the SMA main chain, which may eventually be forced into the PA6 phase from the interface and loses its

expected role as a compatibilizer. Too low an MA concentration has the advantage of not producing the excessive graft copolymer, but tends to produce smaller numbers of the desirable SMA-g-PA6 copolymers and leaves a greater fraction of the unreacted free SMA in the PPO phase. A study of the effect of MA concentration in the SMA copolymer on the efficiency of compatibilization is in progress. We believe that SMA containing 8% MA is probably the best compromise in the one-step blending system. If a two-step sequential blending is carried out by preblending SMA with PA6, then followed by PPO, formation of excessively grafted copolymer is expected to occur.

Since the difference between T_g of PPO and T_m of PA6 is not very great, a certain fraction of the originally added SMA may be mixed within the PA6 phase. It certainly has the first opportunity to react with PA6 to form various degrees of grafted SMA-g-PA6 copolymers in the PA6 phase. When the extent of grafting is still relatively smaller, the lightly grafted SMA-g-PA6 copolymers in the PA6 phase can still migrate into the interface and have their SMA segment diffused into the PPO phase. A portion of the SMA distributed in the PA6 phase may not have the chance to migrate to the interface; additional graft reactions may continue and result in the undesirable excessively grafted copolymer. Such copolymers have the SMA main chain effectively shielded off by the PA6 grafting chains and will eventually reside within the PA6 phase. The key factor in determining the efficiency of a reactive compatibilizer is the extent to which the added copolymer turns into lightly grafted copolymers anchoring along the interface. It appears that a reasonable amount of the SMA copolymer has been able to convert into desirable SMA-g-PA6 copolymers anchoring at the interface and to function as an effective compatibilizer for PA6/PPO blends.

CONCLUSIONS

Polyblends of PA6 and PPO are immiscible and incompatible, with poor interfacial adhesion and large phase domains. This commercially available SMA copolymer has been demonstrated to be a highly effective compatibilizer for PA6/PPO blends. The *in situ*-formed SMA-g-PA6 copolymer tends to anchor along the interface to function as an effective compatibilizer by reducing the interfacial tension and enhancing the interfacial adhesion. The domain size of the compatibilized PA6/PPO blend is reduced with increasing content of SMA compatibilizer. A substantial decrease of the glass transition temperature of the PPO after compatibilization indicates that a certain fraction of the unreacted free SMA is dissolved in the PPO phase. PA6 is in a co-continuous structure with PPO in this PPO-rich uncompatibilized blend (PA6/PPO = 30/70) but tends to shift into a continuous matrix after SMA compatibilization. The overall improvement in mechanical properties is drastic after compatibilization, especially for PPO-rich blends.

ACKNOWLEDGEMENT

This research project was financially supported by the National Science Council of the Republic of China under contract number NSC85-2216-E009-001.

REFERENCES

1. Campbell, J. R., Hobbs, S. Y., Shea, T. J. and Watkins, V. H., *Polym. Eng. Sci.*, 1990, **30**, 1056.
2. Koning, C. and Vondervoort, L. V. D., in *ANTEC'92*, 1992, p. 1435.
3. Hobbs, S. Y., Dekkers, M. E. J. and Watkins, V. H., *J. Mater. Sci.*, 1989, **24**, 2025.
4. Hobbs, S. Y. and Dekkers, M. E. J., *J. Mater. Sci.*, 1989, **24**, 1316.
5. Nishio, T., Sanada, T. and Okada, T., US Patent No. 5 159 018, 1992.
6. Nishio, T., Kuribayashi, H. and Sanada, T., US Patent No 5 237 002, 1993.
7. Nishio, T., Sanada, T. and Satoru, H., US Patent No. 5 262 478, 1993.
8. Gallucci, R. R., US Patent No. 5 260 374, 1993.
9. Laverty, J. J., Ellis, T., Ogara, J. and Kim, S., *Polym. Eng. Sci.*, 1996, **36**, 347.
10. Ghidoni, D., Bencini, E. and Nocci, R., *J. Mater. Sci.*, 1996, **31**, 95.
11. Akkapeddi, M. K., Buskirk, B. V. and Dege, G. J., in *ANTEC'94*, 1994, p. 1509.
12. Lai, Y. C., *J. Appl. Polym. Sci.*, 1994, **54**, 1289.
13. Chiang, C. R. and Chang, F. C., *J. Appl. Polym. Sci.*, 1996, **61**, 2411.
14. Suzuki, K. and Ono, S., Japanese Patent No. 60-155259, 1985.
15. Kasahara, H., Fukuda, K. and Suzuki, H., Japanese Patent No. 57-36150, 1982.
16. Yamahsita, I., Kasahara, H. and Fukuda, K., Japanese Patent No. 57-165448, 1982.
17. Scott, C. and Macosko, C., *J. Polym. Sci., Part B*, 1994, **32**, 205.
18. Galord, N. G., in *Reactive Extrusion: Principles and Practice*, ed. M. Xanthos, Hanser, Munich, 1992.
19. Pavia, D. L., Lampmam, G. M. and Kriz, G. S., *Introduction to Spectroscopy: A Guide for Students of Organic Chemistry*, Saunders, College Publishing, Philadelphia, 1979.
20. Fried, J. R. and Hanna, G. A., *Polym. Eng. Sci.*, 1982, **22**, 705.
21. Witteler, H., Leiser, G. and Droscher, M., *Makromol. Chem. Rapid Commun.*, 1993, **14**, 401.
22. Holsti-Miettinen, R. and Seppala, J., *Polym. Eng. Sci.*, 1992, **32**, 686.
23. Peiffer, D. G. and Rabeony, M., *J. Appl. Polym. Sci.*, 1994, **51**, 1283.
24. Maa, C. T. and Chang, F. C., *J. Appl. Polym. Sci.*, 1993, **49**, 913.
25. Chang, H. H., Wu, J. S. and Chang, F. C., *J. Polym. Res.*, 1994, **1**, 235.